Optical trapping using cascade conical refraction of light

D. P. O'Dwyer,[1] K. E. Ballantine,[1] C. F. Phelan,[1] J. G. Lunney,[1,2] and J. F. Donegan[1,2,*]

[1]*School of Physics, Trinity College Dublin, Dublin 2, Ireland*
[2]*Centre for Research on Adaptive Nanostructures and Nanodevices (CRANN), Trinity College Dublin, Dublin 2, Ireland*
[*]*jdonegan@tcd.ie*

Abstract: Cascade conical refraction occurs when a beam of light travels through two or more biaxial crystals arranged in series. The output beam can be altered by varying the relative azimuthal orientation of the two biaxial crystals. For two identical crystals, in general the output beam comprises a ring beam with a spot at its centre. The relative intensities of the spot and ring can be controlled by varying the azimuthal angle between the refracted cones formed in each crystal. We have used this beam arrangement to trap one microsphere within the central spot and a second microsphere on the ring. Using linearly polarized light, we can rotate the microsphere on the ring with respect to the central sphere. Finally, using a half wave-plate between the two crystals, we can create a unique beam profile that has two intensity peaks on the ring, and thereby trap two microspheres on diametrically opposite points on the ring and rotate them around the central sphere. Such a versatile optical trap should find application in optical trapping setups.

OCIS codes: (140.7010) Laser trapping; (050.1940) Diffraction; (260.1440) Crystal optics.

References and links

1. W. R. Hamilton, "Third supplement to an essay on the theory of system of rays," Trans. R. Irish Acad. **17**, 1–144 (1837).
2. H. Lloyd, "On the phenomena presented by light in its passage along the axes of biaxial crystals," Philos. Mag. **1**, 112–120 (1833).
3. A. M. Belskii and A. P. Khapaluyk, "Internal conical refraction of bounded light beams in biaxial crystals," Opt. Spectrosc. **44**, 312–315 (1978).
4. M. V. Berry, "Conical refraction asymptotics: fine structure of Poggendorff rings and axial spike," J. Opt. A, Pure Appl. Opt. **6**(4), 289–300 (2004).
5. C. F. Phelan, D. P. O'Dwyer, Y. P. Rakovich, J. F. Donegan, and J. G. Lunney, "Conical diffraction and Bessel beam formation with a high optical quality biaxial crystal," Opt. Express **17**(15), 12891–12899 (2009).
6. D. P. O'Dwyer, C. F. Phelan, Y. P. Rakovich, P. R. Eastham, J. G. Lunney, and J. F. Donegan, "Generation of continuously tunable fractional optical orbital angular momentum using internal conical diffraction," Opt. Express **18**(16), 16480–16485 (2010).
7. V. Peet, "Biaxial crystal as a versatile mode converter," J. Opt. **12**(9), 095706 (2010).
8. A. Ashkin, J. M. Dziedzic, J. E. Bjorkholm, and S. Chu, "Observation of a single-beam gradient force optical trap for dielectric particles," Opt. Lett. **11**(5), 288–290 (1986).
9. A. Ashkin, J. M. Dziedzic, and T. Yamane, "Optical trapping and manipulation of single cells using infrared laser beams," Nature **330**(6150), 769–771 (1987).
10. K. Dholakia and T. Čižmár, "Shaping the future of manipulation," Nat. Photonics **5**(6), 335–342 (2011).
11. M. Padgett and R. Bowman, "Tweezers with a twist," Nat. Photonics **5**(6), 343–348 (2011).
12. N. B. Simpson, K. Dholakia, L. Allen, and M. J. Padgett, "Mechanical equivalence of spin and orbital angular momentum of light: An optical spanner," Opt. Lett. **22**(1), 52–54 (1997).
13. K. Volke-Sepúlveda, S. Chavez-Cerda, V. Garces-Chavez, and K. Dholakia, "Three-dimensional optical forces and transfer of orbital angular momentum from multiringed light beams to spherical microparticles," J. Opt. Soc. Am. B **21**, 1749–1757 (2004).
14. R. Bowman, A. Jesacher, G. Thalhammer, G. Gibson, M. Ritsch-Marte, and M. Padgett, "Position clamping in a holographic counterpropagating optical trap," Opt. Express **19**(10), 9908–9914 (2011).

#172917 - $15.00 USD Received 19 Jul 2012; revised 20 Aug 2012; accepted 20 Aug 2012; published 30 Aug 2012

15. E. McLeod and C. B. Arnold, "Array-based optical nanolithography using optically trapped microlenses," Opt. Express **17**(5), 3640–3650 (2009).
16. K. Visscher, S. P. Gross, and S. M. Block, "Construction of multiple-beam optical traps with nanometer-resolution position sensing," IEEE J. Sel. Top. Quantum Electron. **2**(4), 1066–1076 (1996).
17. K. Sasaki, M. Koshioka, H. Misawa, N. Kitamura, and H. Masuhara, "Laser-scanning micromanipulation and spatial patterning of fine particles," Jpn. J. Appl. Phys. **30**(Part 2, No. 5B), L907–L909 (1991).
18. M. Capitanio, R. Cicchi, and F. S. Pavone, "Continuous and time-shared multiple optical tweezers for the study of single motor proteins," Opt. Lasers Eng. **45**(4), 450–457 (2007).
19. E. Martín-Badosa, M. Montes-Usategui, A. Carnicer, J. Andilla, E. Pleguezuelos, and I. Juvells, "Design strategies for optimizing holographic optical tweezers set-ups," J. Opt. A **9**(8), S267–S277 (2007).
20. D. P. O'Dwyer, C. F. Phelan, K. E. Ballantine, Y. P. Rakovich, J. G. Lunney, and J. F. Donegan, "Conical diffraction of linearly polarised light controls the angular position of a microscopic object," Opt. Express **18**(26), 27319–27326 (2010).
21. M. V. Berry, "Conical diffraction from an N-crystal cascade," J. Opt. **12**(7), 075704 (2010).
22. A. Abdolvand, K. G. Wilcox, T. K. Kalkandjiev, and E. U. Rafailov, "Conical refraction Nd:KGd(WO_4)$_2$ laser," Opt. Express **18**(3), 2753–2759 (2010).
23. D. P. O'Dwyer, C. F. Phelan, Y. P. Rakovich, P. R. Eastham, J. G. Lunney, and J. F. Donegan, "The creation and annihilation of optical vortices using cascade conical diffraction," Opt. Express **19**(3), 2580–2588 (2011).
24. C. F. Phelan, K. E. Ballantine, P. R. Eastham, J. F. Donegan, and J. G. Lunney, "Conical diffraction of a Gaussian beam with a two crystal cascade," Opt. Express **20**, 13201–13207 (2012).

1. Introduction

Conical refraction of light was predicted by Hamilton and demonstrated by Lloyd in one of the earliest theoretical predictions that was followed by an experimental demonstration [1, 2]. In internal conical refraction, a beam of light refracted along one of the optic axes of a slab of biaxial crystal, propagates as a slant hollow cone of light inside the crystal. Upon exiting the crystal, this cone is refracted into a ring-shaped beam that propagates in the same direction as the incident beam. Hamilton's geometrical optics description has been extended to the paraxial wave optics theory of conical diffraction by Berry and others [3, 4] and the agreement with experimental results is excellent [5–7]. The ring-shaped beam is most sharply defined at the position known as the focal image plane (FIP).

Optical traps are used in a wide variety of experimental setups from basic studies of atom dynamics to biological cell stretching studies. The early work owes much to the insight of Ashkin and his associates who led off this research area in 1986 [8, 9]. Traps are now routinely used to optically manipulate micron-scale objects in physics, chemistry and biology. Recent reviews of the field of optical trapping describe the large range of areas to which trapping has been applied and suggest future developments [10, 11]. There is now a great deal of sophistication in the geometry of the optical trap since beams can be produced and altered using a wide range of optical devices. Various trap arrangements have been studied in which optical orbital angular momentum, in addition to linear optical momentum, is used to manipulate microscopic objects [12, 13]. Counter-propagating beams are used to improve the stiffness of the trap, while, by using two or more laser frequencies, it is possible to manipulate a trapped microsphere and write nanoscale features on a surface [14, 15]. Of particular note is the use of spatial light modulation techniques to make an array of traps and so manipulate a whole assembly of particles [16–19]. In a recent study, we have shown how conical refraction of linearly polarized light beam can be used to control the angular position of a trapped microsphere, thereby adding to the panoply of techniques for optical manipulation studies [20]. In this study, using cascade conical diffraction, we can form a unique optical profile consisting of a ring-shaped beam with a central Gaussian spot which offers new functionality for optical trapping and manipulation.

2. Cascade conical refraction of light

Internal conical refraction of light occurs in a biaxial crystal when a narrow beam of light is incident on a slab of biaxial crystal such that the beam is refracted along one of the optic axes. The beam propagates as a slant cone of rays inside the crystal and emerges as a hollow

#172917 - $15.00 USD Received 19 Jul 2012; revised 20 Aug 2012; accepted 20 Aug 2012; published 30 Aug 2012

cylindrical beam. If the principal refractive indices are $n_1<n_2<n_3$, the semi-angle A of the slant cone is given by:

$$A=\frac{1}{n_2}\sqrt{(n_3-n_2)(n_2-n_1)} \tag{1}$$

and the radius of the ring-shaped beam at the focal image plane (FIP) is given by $R_0 = AL$, where L is the length of the crystal, as depicted in Fig. 1. The FIP is the spatial position where the rings are at their sharpest occurring at the equivalent incident beam waist position. The refracted ring of light is in fact a double ring of light separated by a dark ring, known as the Poggendorff ring. The ring radius R_0 is the radius of the Poggendorff dark ring, and occurs due to the circularly symmetric double refraction of the light around R_0 [4].

In dealing with cascade conical refraction, it is necessary to specify the relative azimuthal orientation of the different crystals, with respect to the axis defined by the direction of propagation of the light. To do this we define a second direction, in addition to the optic axis, in the biaxial crystal. Here we take γ to be perpendicular to the optic axis and in the direction of the displacement of the center of the ring beam from the line of propagation of the ray which is refracted in the ordinary manner, which is simply identified by being polarized tangential to the ring. The relative angle between successive crystals directly affects the final intensity profile.

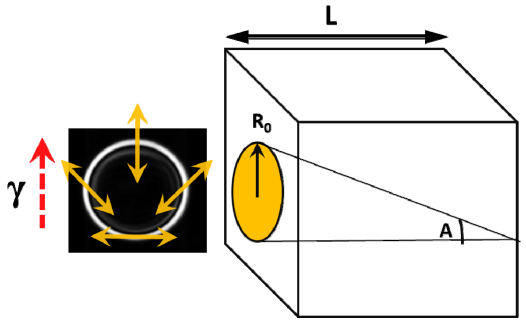

Fig. 1. Schematic of conical refraction. A beam traversing a crystal of length (L) is refracted through a semi-angle (A) to give a ring radius of R_0. The beam shift direction (γ) is in the direction of the parallel polarization component towards the orthogonally polarized component at the opposite side of the ring.

When a Gaussian light beam propagates through two identical biaxial crystals in cascade with optical axes and γ aligned parallel the output beam is ring-shaped with a radius twice that obtained for a single crystal. If the angle α between the beam shift directions is 180°, a ring profile is generated following the first crystal, and after this propagates through the second crystal the ring beam is converted back to the original Gaussian spot. For values of α between zero and 180°, the beam profile after conical diffraction in the two crystals is ring-shaped with a Gaussian spot at the centre. The relative intensity of the Gaussian and the ring can be adjusted by changing the angle α. The effect of propagating a Gaussian beam along the optic axes of N biaxial crystals have been investigated theoretically by Berry [21]. Two-crystal cascade conical refraction has been used in the construction of a high efficiency optically pumped laser [22]. We have studied the creation and annihilation of optical vortices in cascade conical refraction using careful manipulation of the polarization between successive biaxial crystals [23]. In a recent study, we have experimentally investigated cascade conical refraction for two crystals, of equal and unequal lengths, and shown that the results are in good agreement with the paraxial theory of conical refraction [24].

#172917 - $15.00 USD Received 19 Jul 2012; revised 20 Aug 2012; accepted 20 Aug 2012; published 30 Aug 2012

3. Experimental setup

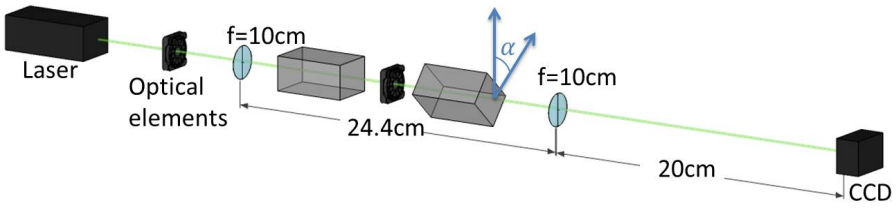

Fig. 2. Experimental setup for observation of focal image plane profiles. The two biaxial crystals are located between the two lenses, one rotated at an angle α around the beam axis; optical elements can be placed after the laser or in between the crystals and include linear polarizer, quarter or half wave-plate, or some combination of these.

The biaxial crystals used were slabs of $KGd(WO_4)_2$ obtained from *CROptics* with dimensions of 4.0 x 3.0 x 21.1 mm and 4.0 x 3.0 x 20.9 mm respectively. The principal refractive indices of the crystals were $n_1 = 2.013$, $n_2 = 2.045$, $n_3 = 2.086$ for a wavelength of 632.8 nm. This implies that the semi-angle of the cone of rays in the crystal $A = 0.0177$ rad and the ring radius for propagation through each of the crystals is $R_{01} = 0.374$ mm and $R_{02} = 0.370$ mm respectively. The laser used was a circularly-polarized 10 mW He-Ne focused to a 45μm waist, $w_{0,}$ using a converging lens with 10 cm focal length. For internal conical diffraction the ring beam is most sharply defined at the FIP, which corresponds to the image of the Gaussian beam waist in the crystal. We can define a parameter $\rho_0 = R_0/w_0$ which determines the sharpness of the fine structure in the radial irradiance distribution in the FIP. A converging lens was used to form an image of the FIP, with unit magnification, on a 2-dimensional CCD, as shown in Fig. 2.

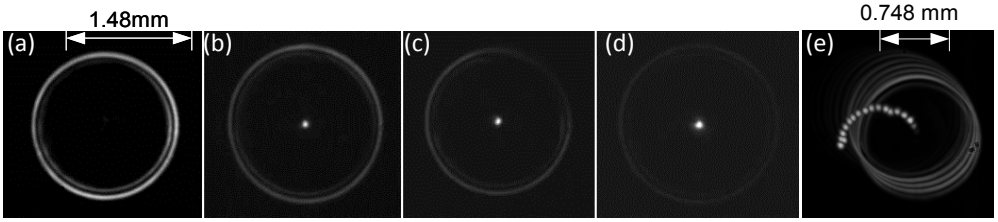

Fig. 3. CCD images of the FIP with (a) α = 0°,(b) α = 20°, (c) α = 45°, (d) α = 90°. (e) Processed image of all frames from α = 0 to 180°. The path of the Gaussian central spot travels along the patch of the ring generated from the first crystal and increases in intensity. is

Figure 3 shows CCD images of the FIP profile for a range of values of α, the relative azimuthal orientation of the two biaxial crystals. The transition from double ring beam to Gaussian spot can clearly be seen. At $\alpha = 0$, the central spot is absent. For an angle of 20°, the spot is clearly observed together with the ring, and as α is further increased the optical power in the ring declines relative the spot. For sufficiently large values of ρ_0 the ring and spot distributions will not overlap; as is the case in Fig. 2, where $\rho_{01} = 8.3$ and $\rho_{02} = 8.2$. In that case it can be shown the optical power of the spot relative to the ring is given by $(1-\cos\alpha)/(1+\cos\alpha)$ [21]. It should be noted that as α is varied by rotating the second crystal the ring and spot rotate together on a circle with a radius equal to R_{02}. As the crystals are rotated with respect to each other, the path of the Gaussian spot rotates on a path matching that of the ring formed by the 1st crystal, as shown in Fig. 3(e). In the experiments below we fix the angle α to define the power ratio between the rings and spot.

#172917 - $15.00 USD Received 19 Jul 2012; revised 20 Aug 2012; accepted 20 Aug 2012; published 30 Aug 2012

4. Experimental results for optical trapping

Figure 4 shows the optical setup for optical trapping using cascade conical diffraction beam, using a Gaussian beam from a 532 nm Nd-YAG CW. The laser is focused using a 10 cm focal length converging lens (L_1) to a beam waist with a $1/e^2$ radius of 37 μm. . At 532 nm the refractive indices are n_1 = 2.031, n_2 = 2.063, n_3 = 2.118, with a cone angle A = 0.02024 radians. The resulting ring radii are R_{01} = 0.428 mm and R_{02} = 0.431 mm and R_{01+02} = 0.859mm. This results in ρ_{01} = 11.56, ρ_{02} = 11.64 and ρ_{01+02} = *23.20*. Both linearly and circularly polarised light are used. This beam propagates through two almost identical biaxial crystals with optic axes aligned parallel. The second crystal is rotated about the optic axis to adjust the angle α between the displacement directions of the two crystals and so vary the optical power ratio between the centre spot and the rings in the FIP. The irradiance distribution in the FIP plane is imaged to the sample plane of the microscope with demagnification determined by the lens L_2 and the objective L_3. The diameter D_t of the outermost ring in the sample plane is:

$$D_t = 2\frac{f_3(R_{01}+R_{02})}{f_2}. \qquad (2)$$

For f_2 = 22 cm and f_3 = 1.81 mm (Leitz Neoplan Fluotar 100 × 0.9NA objective), the dark ring has a diameter D_t = 12.4 μm. This beam was used to trap polystyrene microspheres suspended in water. Polystyrene spheres of either 5.2 μm or 2.8 μm diameter are used and both have refractive index n = 1.55. A drop of the microsphere suspension is sealed between two microscope cover slips using Vaseline around the edges. To measure the optical power in the trap, the sample holder is replaced by an optical power meter.

4.1 Linearly polarized input beam

With linearly polarised light entering the first crystal, the emerging beam from the cascade consists of a crescent with a bright spot at the centre, as shown in Fig. 5. By rotating the plane of linear polarisation of light incident on the cascade, the position of the maximum irradiance of the crescent rotates around the ring. Using this beam, it is possible to trap one particle in the high intensity spot in the centre and have another particle orbit around it. Frames from such an orbit of trapped 5.2 μm diameter spheres are shown in Fig. 6. Note that there is some movement of the centre particle. The maximum deviation of the centre of this particle from its average position is about 1.2 μm. Media 1 shows the rotation of the microsphere trapped on the ring with respect to the microsphere trapped at the centre of the beam.

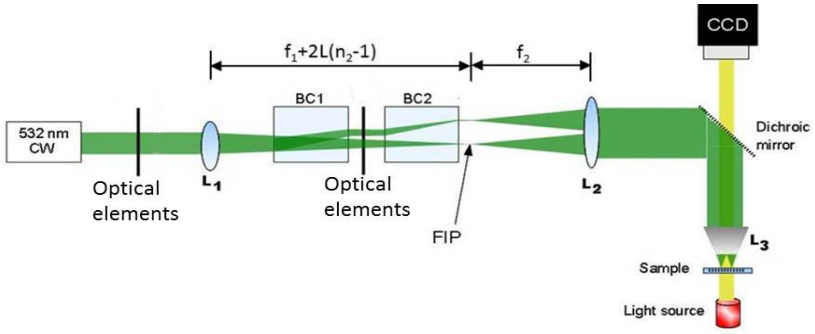

Fig. 4. Optical setup for cascade conical diffraction optical trap. The dichroic mirror prevents the 532 nm trapping beam entering the CCD. Sample illumination for CCD recording is provided by the light source below the sample. Optical elements can include linear polarizer, quarter or half wave-plate, or some combination.

#172917 - $15.00 USD Received 19 Jul 2012; revised 20 Aug 2012; accepted 20 Aug 2012; published 30 Aug 2012

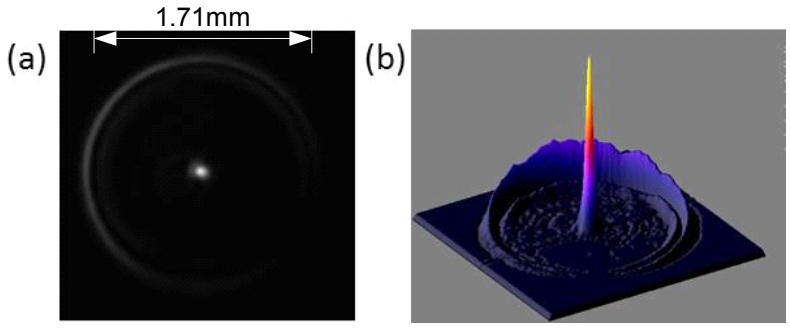

Fig. 5. (a) Intensity profile of cascade conical refraction beam in the FIP with linearly polarized 532nm light incident on the first crystal. (b) 3-D plot of the intensity distribution in (a).

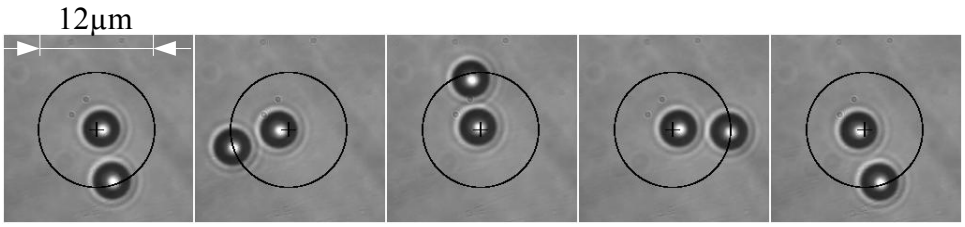

Fig. 6. Several individual frames showing how a particle trapped in the crescent beam orbits around the particle trapped in central beam spot. Media 1 shows the rotation of the outer microsphere with respect to the centrally trap microsphere as the plane of polarization of the incident beam is rotated.

4.2 Half wave-plate located between the two crystals

A beam with crescent–shaped intensity distributions on either side of a central spot is obtained by placing a half wave-plate between the two crystals, as shown in Fig. 7. For this experiment, the input light is circularly polarized and the beam is rotated by rotating the half wave-plate between the crystals. As before, the crescent-shaped lobes can be rotated around the central beam spot by rotating half wave-plate between the crystals [24]. This beam profile was used to trap three particles in a line, and rotate the outer two around the central particle while keeping them diametrically opposed, as shown in Fig. 8 and in Media 2. Particles rotate anti-clockwise. They move slightly away from being on a straight line due to small intensity variations in the beam profile.

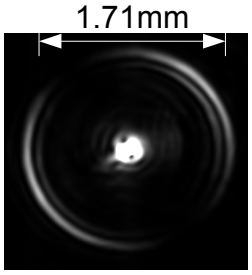

Fig. 7. Beam profile in the FIP with a half-wave plate between the two biaxial crystals.

#172917 - $15.00 USD Received 19 Jul 2012; revised 20 Aug 2012; accepted 20 Aug 2012; published 30 Aug 2012

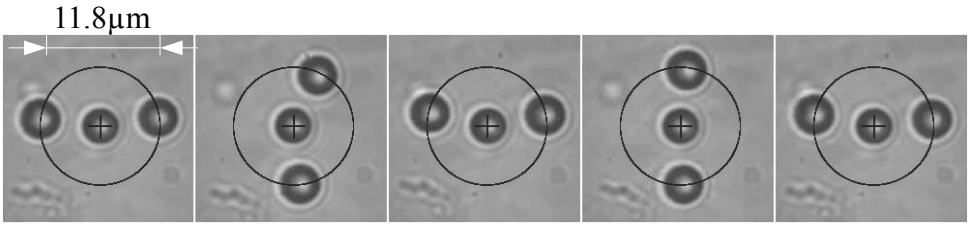

Fig. 8. Frames from rotation of two diametrically opposed particles trapped in lobes around a stationary particle trapped in the centre. Media 2 shows the continuous anti-clockwise rotation of the two microparticles around the central particle trapped in the Gaussian spot.

4.3 Characterisation of optical trap

The maximum trapping force on the particle trapped in either the ring or the central spot was measured by moving the sample at increasing speeds until the particle escapes. The maximum force F is related to this maximum speed v by Stokes' law:

$$F = 6\pi R_p \eta v, \tag{3}$$

where R_p is the radius of the particle and η is the viscosity of the water. The input beam was circularly polarised and used to produce a beam of the form shown in Fig. 3, and the value of α was varied to change the relative intensity of the ring and the central spot. The maximum force is found to be proportional to the total power in the beam, P, and the strength of the trap can be expressed by the dimensionless parameter Q, which is the fraction of the linear optical momentum transferred to the particle; $F = QnP/c$. The force was measured for powers ranging up to 200 mW. A typical measurement, for $\alpha = 20°$ and $P = 97$ mW, results in maximum forces of 1.86 pN in the central spot and 1.37 pN in the ring, which corresponds to $Q = 0.0043$ and 0.0032 for the spot and ring. Note that only a small fraction of the overall power in the ring is used to trap the particle held there.

5. Conclusions

In conclusion, we have developed a novel optical trap based on cascade conical refraction where two biaxial crystals are arranged in series with their optical axes aligned. Then for circularly polarized input the output beam is ring-shaped with a central spot. The relative intensity of the spot and ring may be altered by varying the azimuthal angle between the slant cones in the two crystals. For linearly polarized light the ring is reduced to a crescent, and this beam has been used to trap one microsphere on the ring and a second in the centre. The particle on the ring may be rotated by simply rotating the incident linear polarization. An extension of the arrangement, whereby two particles were trapped at diametrically opposed positions on the ring, was also demonstrated. These new optical beam shapes should find application where simultaneous trapping of two or more particles is required and where optical rotation is needed, as in optical motors.

Acknowledgments

We acknowledge the financial support of Science Foundation Ireland SFI under grant number 08/IN.1/I1862.

#172917 - $15.00 USD Received 19 Jul 2012; revised 20 Aug 2012; accepted 20 Aug 2012; published 30 Aug 2012